RSC Advances

PAPER

View Article Online
View Journal | View Issue

Cite this: *RSC Adv.*, 2021, **11**, 37011

Evaluation of enzymatic and magnetic properties of γ-glutamyl-[1-^{13}C]glycine and its deuteration toward longer retention of the hyperpolarized state†

Yohei Kondo, [a] Yutaro Saito, [a] Abdelazim Elsayed Elhelaly,[b] Fuminori Hyodo,[b] Tatsuya Nishihara,‡[a] Marino Itoda,[a] Hiroshi Nonaka, §[a] Masayuki Matsuo[c] and Shinsuke Sando *[ad]

Dynamic nuclear polarization (DNP) is an emerging cutting-edge method of acquiring metabolic and physiological information *in vivo*. We recently developed γ-glutamyl-[1-^{13}C]glycine (γ-Glu-[1-^{13}C]Gly) as a DNP nuclear magnetic resonance (NMR) molecular probe to detect γ-glutamyl transpeptidase (GGT) activity *in vivo*. However, the detailed enzymatic and magnetic properties of this probe remain unknown. Here, we evaluate a γ-Glu–Gly scaffold and develop a deuterated probe, γ-Glu-[1-^{13}C]Gly-d_2, that can realize a longer lifetime of the hyperpolarized signal. We initially evaluated the GGT-mediated enzymatic conversion of γ-Glu–Gly and the magnetic properties of ^{13}C-enriched γ-Glu–Gly (γ-Glu-[1-^{13}C]Gly and γ-[5-^{13}C]Glu–Gly) to support the validity of γ-Glu-[1-^{13}C]Gly as a DNP NMR molecular probe for GGT. We then examined the spin-lattice relaxation time (T_1) of γ-Glu-[1-^{13}C]Gly and γ-Glu-[1-^{13}C]Gly-d_2 under various conditions (D_2O, PBS, and serum) and confirmed that the T_1 of γ-Glu-[1-^{13}C]Gly and γ-Glu-[1-^{13}C]Gly-d_2 was maintained for 30 s (9.4 T) and 41 s (9.4 T), respectively, even in serum. Relaxation analysis of γ-Glu-[1-^{13}C]Gly revealed a significant contribution of the dipole–dipole interaction and the chemical shift anisotropy relaxation pathway (71% of the total relaxation rate at 9.4 T), indicating the potential of deuteration and the use of a lower magnetic field for realizing a longer T_1. In fact, by using γ-Glu-[1-^{13}C]Gly-d_2 as a DNP probe, we achieved longer retention of the hyperpolarized signal at 1.4 T.

Received 2nd October 2021
Accepted 11th November 2021

DOI: 10.1039/d1ra07343e

rsc.li/rsc-advances

Introduction

The cell surface-bound enzyme γ-glutamyl transpeptidase (GGT) catalyzes a reaction that initiates the cellular uptake of the biological antioxidant glutathione (GSH).[1] The γ-glutamyl group of its natural substrate GSH is accurately recognized by GGT, and the γ-peptide bond is hydrolyzed or glutamic acid (Glu) is transferred to acceptors such as amino acids and peptides. The resulting cysteinyl–glycine (Cys–Gly) undergoes further metabolism by dipeptidases to generate cysteine (Cys) and glycine (Gly). These amino acids are then taken up by cells and resynthesized into intracellular GSH.[2] Thus, GGT is an important enzyme involved in the redox state through GSH homeostasis *in vivo*. In particular, GGT is abundantly expressed in cancers such as soft tissue sarcoma and ovarian adenocarcinoma.[3] Thus, GGT could be a useful cancer biomarker, and the detection of GGT expression and its activity *in vivo* are of biological and medical importance.

The expression and activity of GGT have been detected using various detection modalities. For example, GGT expression *in vivo* can be visualized using positron emission tomography (PET),[4,5] but this approach cannot directly detect GGT activity. Fluorescent molecular probes for detecting GGT activity have been extensively studied, and some have been applied to fluorescence-guided surgery.[6,7] Furthermore, molecular imaging *in vivo* using hyperpolarization has recently attracted attention because it significantly improves the sensitivity of nuclear magnetic resonance and imaging (NMR/MRI).[8]

[a]*Department of Chemistry and Biotechnology, Graduate School of Engineering, The University of Tokyo, 7-3-1 Hongo, Bunkyo-ku, Tokyo 113-8656, Japan. E-mail: ssando@chembio.t.u-tokyo.ac.jp*

[b]*Department of Radiology, Frontier Science for Imaging, School of Medicine, Gifu University, 1-1 Yanagido, Gifu 501-1194, Japan*

[c]*Department of Radiology, School of Medicine, Gifu University, 1-1 Yanagido, Gifu 501-1194, Japan*

[d]*Department of Bioengineering, Graduate School of Engineering, The University of Tokyo, 7-3-1 Hongo, Bunkyo-ku, Tokyo 113-8656, Japan*

† Electronic supplementary information (ESI) available. See DOI: 10.1039/d1ra07343e

‡ Present address: Department of Chemistry and Biological Science, College of Science and Engineering, Aoyama Gakuin University, 5-10-1 Fuchinobe, Chuo-ku, Sagamihara, 252-5258, Japan.

§ Present address: Department of Synthetic Chemistry and Biological Chemistry, Graduate School of Engineering, Kyoto University, Kyoto University Katsura, Nishikyo-ku, 615-8510, Japan.

Dissolution dynamic nuclear polarization (d-DNP) is a reliable method of hyperpolarization that can increase the detection sensitivity of ^{13}C-enriched biomolecules, including ^{13}C-pyruvic acid, and acquire physiological information about metabolism and pH *in vivo*.[9,10] DNP NMR using ^{13}C-pyruvic acid has also been clinically applied to detect human prostate cancers, indicating the medical and biological value of DNP NMR.[11,12]

We recently developed γ-glutamyl-[1-^{13}C]glycine (γ-Glu-[1-^{13}C]Gly) as a DNP NMR molecular probe to non-invasively detect GGT activity *in vivo* (Fig. 1).[13] The structure of γ-Glu-[1-^{13}C]Gly comprises a γ-Glu group as a GGT recognition moiety and [1-^{13}C]Gly as a signaling moiety. The γ-Glu-[1-^{13}C]Gly probe was converted to the product, [1-^{13}C]Gly, by an enzymatic reaction with GGT. The ^{13}C chemical shift change between the probe and the product was 4.3 ppm, which is large enough to distinguish *in vivo*. The spin-lattice relaxation time (T_1) correlates with the retention time of the hyperpolarized state, and the probe and product had sufficiently long T_1 values of 30 s (9.4 T, H_2O) and 45 s (9.4 T, H_2O), respectively, to detect GGT activity in rat kidneys. Since then, γ-Glu-[1-^{13}C]Gly has been applied in studies of rat kidneys function, subcutaneous ovarian carcinoma, and MiaPaCa-2 xenografts, as well as glioma models, and it should have further applications *in vivo*.[14–17] However, the structure–activity relationship and detailed magnetic parameters of γ-Glu-[1-^{13}C]Gly, which are important for DNP MRI studies, have not been investigated.

Here, we report an evaluation of the enzymatic and magnetic properties of γ-Glu-[1-^{13}C]Gly and the development of a deuterated probe, γ-Glu-[1-^{13}C]Gly-d_2, that can achieve longer lifetime of the hyperpolarized signal than the conventional probe.

Experimental

Synthesis

General remarks. Reagents and solvents were purchased from standard suppliers and used without further purification. NMR spectra for characterization were acquired with a JNM-ECS 400 spectrometer (^{1}H: 400 MHz, ^{13}C: 100 MHz, JEOL, Japan). All chemical shifts are reported in parts per million (ppm) relative to internal standard. Chloroform-d_1 (δ 7.26 ppm) or D_2O (δ 4.79 ppm) were used as internal standards for ^{1}H NMR. Chloroform-d_1 (δ 77.2 ppm) or 1,4-dioxane (δ 67.2 ppm) in D_2O were used as internal standards for ^{13}C NMR. Data are reported as follows: chemical shift, multiplicity (s = singlet, brs = broad singlet, d = doublet, t = triplet, m = multiplet), coupling constant (Hz), and integration. High resolution mass spectrometry (HRMS) was acquired using micrOTOF II (ESI, Bruker Daltonics, USA).

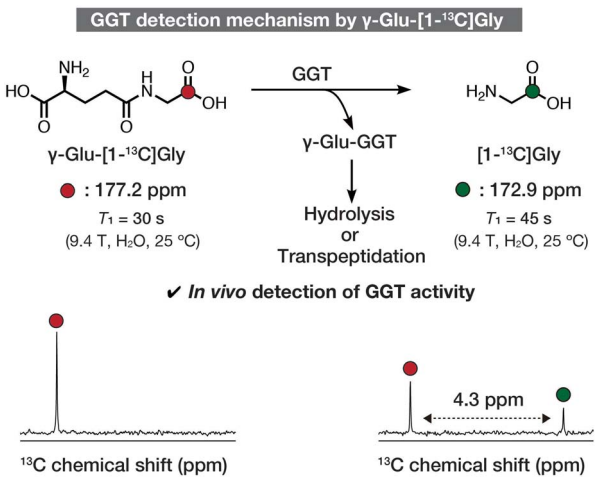

Fig. 1 Schematic illustration of detection of GGT using γ-Glu-[1-^{13}C]Gly. ^{13}C Chemical shift and T_1 values are cited from ref. 13. Colored atoms indicate isotope-enriched ^{13}C.

Synthesis of *N*-Cbz-γ-Glu(OBn)-OSu. To a three-necked 300 mL round-bottom flask with a magnetic stirring bar, *N*-Cbz-γ-Glu(OBn) (6.00 g, 16.2 mmol) was added. The vessel was heated under vacuum for 10 min to remove water. After cooling to room temperature, *N*-hydroxyl succinimide (NHS, 3.72 g, 32.4 mmol, 2.0 equiv.) and 4-dimethylaminopyridine (DMAP, 103 mg, 841 μmol, 5.2 mol%) were added. The vessel was purged with N_2 through evacuation and filling back N_2 three times. After adding DMF (70 mL) and 1-ethyl-3-(3-dimethylaminopropyl)carbodiimide hydrochloride (EDCI·HCl, 4.65 g, 24.2 mmol, 1.5 equiv.), the mixture was stirred at room temperature for 36 h under N_2 atmosphere. The resulting mixture was added EtOAc (140 mL), and washed with water (200 mL × 4) and brine (60 mL × 3). The resulting solution was dried over anhydrous Na_2SO_4, filtered, and concentrated under reduced pressure. The desired compound was obtained (7.49 g, 99% yield) by recrystallization from hexane/$CHCl_3$ as a colorless crystal. Characterization was conducted according to the previous literature.[18]

Synthesis of *N*-Cbz-γ-Glu(OBn)-[1-^{13}C]Gly-d_2. To a 50 mL round-bottom flask with a magnetic stirring bar, [1-^{13}C]Gly (504 mg, 6.62 mmol), ruthenium on activated carbon (208 mg, 1.6 mol% for Ru), and D_2O (10 mL) were added. The vessel was purged with H_2 through evacuation of air and filling back H_2 three times. The mixture was stirred at 90 °C for 19 h. After cooling to room temperature, the resulting mixture was filtered through Celite®. The filtrate was concentrated under reduced pressure. The product, [1-^{13}C]Gly-d_2, was used for the next step without further purification and characterization.

To a 25 mL round-bottom flask with a magnetic stirring bar, *N*-Cbz-γ-Glu(OBn)-OSu (403 mg, 861 μmol, 1.0 equiv.) was added. After adding THF (2.0 mL), H_2O (2.0 mL), [1-^{13}C]Gly-d_2 (66.8 mg, 856 μmol), and Et_3N (349 μL, 2.50 mmol, 2.9 equiv.), the reaction mixture was stirred at room temperature for 30 min. The resulting mixture was evaporated to remove the solvent. After acidifying with 0.1 M HCl aq., the residue was extracted with EtOAc (30 mL × 2) and washed with 0.1 M HCl aq. (30 mL × 2) and brine (30 mL × 1). The resulting solution was dried over anhydrous Na_2SO_4, filtered, and concentrated under reduced pressure. The residue was subjected to silica-gel column chromatography (CH_2Cl_2/MeOH) to afford *N*-Cbz-Glu(OBn)-[1-^{13}C]Gly-d_2 (305 mg, 83% yield based on [1-^{13}C]Gly-d_2) as a white solid.

^{1}H NMR (400 MHz, $CDCl_3$) δ 7.38–7.29 (m, 10H), 6.50 (brs, 1H), 5.66 (d, J = 7.6 Hz, 1H), 5.21–5.14 (m, 2H), 5.10 (s, 2H), 4.49–4.44 (m, 1H), 4.07–3.94 (m, 0.16H, deuterated), 2.34–2.21 (m, 3H), 2.00–1.91 (m, 1H); ^{13}C NMR (100 MHz, $CDCl_3$) δ 172.7

(^{13}C-labeled), 171.9, 170.9, 156.8, 136.1, 135.3, 128.8, 128.8, 128.5, 128.3, 67.7, 67.5, 53.7, 32.2, 28.8, two carbons are not observed due to overlapping, one carbon is not observed due to peak broadening; HRMS (ESI) *m*/*z* calcd for $C_{21}{}^{13}CH_{22}D_2N_2NaO_7$ $[M + Na]^+$: 454.1635, found 454.1637.

Synthesis of γ-Glu-[1-^{13}C]Gly-d_2. To a 50 mL round-bottom flask with a magnetic stirring bar, *N*-Cbz-γ-Glu(OBn)-[1-^{13}C] Gly-d_2 (290 mg, 671 μmol) and palladium on activated carbon (47.0 mg, 6.6 mol% for Pd) were added. The vessel was purged with N_2 through evacuation and filling back N_2 three times. After adding MeOH (5.0 mL), the vessel was purged with H_2. The reaction mixture was stirred at room temperature for 2 h and filtered with Celite®. The filtrate was concentrated under reduced pressure to afford γ-Glu-[1-^{13}C]Gly-d_2 (137 mg, 99% yield) as a white solid.

^{1}H NMR (400 MHz, D_2O) δ 3.93 (brs, 0.16H, deuterated), 3.83 (t, J = 6.2 Hz, 1H), 2.59–2.46 (m, 2H), 2.25–2.11 (m, 2H); ^{13}C NMR (100 MHz, D_2O) δ 177.4 (^{13}C-labeled), 175.2, 174.7, 54.9, 43.7 (brs, deuterated carbon), 32.1, 26.9, ^{13}C NMR was acquired under the neutral condition by adjusting pD using NaOD aqueous solution; HRMS (ESI) *m*/*z* calcd for $C_6{}^{13}CH_{10}D_2N_2NaO_5$ $[M + Na]^+$: 230.0797, found 230.0799.

Glu production monitoring with UHPLC

To 100 μL of the substrate solution (5 mM of γ-Glu–Gly, γ-Glu–Gly–Gly, and GSH, or 0, 0.3125, 0.625, 1.25, 2.5, and 5.0 mM of Glu in 0.1 M PB as calibration samples) was added GGT enzyme solution (1 U mL^{-1} in 0.1 M PB, 15 μL) or 0.1 M PB (15 μL). The reaction mixtures were incubated at 37 °C for 30 min or 60 min. The reaction was quenched by adding GGT inhibitor solution (10 mM of GGsTop® in DMSO, 5 μL). To the vessel containing 80 μL of 50 mM borate buffer (pH 8.0) containing EDTA (20 mM) and 20 μL of 4-fluoro-7-nitrobenzofurazan (20 mM) solution in acetonitrile was added 20 μL of the enzymatic reaction mixture. The resulting mixture was incubated at 60 °C. The 4-fluoro-7-nitrobenzofurazan labeling reaction was quenched by adding 40 μL of 50 mM HCl aqueous solution. The solution was filtered and used for UHPLC analysis. The concentration of Glu that was produced by GGT-mediated reaction from the substrates was quantified by comparing the fluorescent intensity with that of calibration samples of Glu. One unit of GGT was defined as the amount of the enzyme that generates 1.0 μmol of *p*-nitroaniline from γ-Glu–*p*-nitroanilide per minute at 37 °C (2.5 mM γ-Glu–*p*-nitroanilide in 0.1 M PB).

T_1 measurements

T_1 values were determined by inversion recovery method using JEOL JNM-ECS 400 (9.4 T), JEOL JNM-ECA 500 (11.7 T), and JEOL JNM-ECA 600 (14.1 T). Measurement conditions: D_2O, PBS, or mouse serum containing 10% D_2O, 10 mM of the compounds, 37 °C. pD was adjusted to 7.4 ± 0.1 with DCl aq. or NaOD aq. in D_2O. pH was adjusted to 7.4 ± 0.1 with HCl aq. or NaOH aq. in PBS. For the measurements in PBS, glass capillary containing D_2O was used to get the lock signal. All T_1 measurements were conducted under thermal equilibrium state (n = 3).

NMR measurements for ^{13}C chemical shift

^{13}C chemical shift of probes and products were determined in D_2O using 1,4-dioxane (67.19 ppm) as an internal standard at 9.4 T. Measurement conditions: 5 mM of the substrate, 37 °C, D_2O. pD was adjusted to 7.4 ± 0.1 with DCl aq. or NaOD aq. All measurements were conducted at thermal equilibrium state.

R_{1DD} analysis

^{1}H–^{13}C dipole–dipole (DD) relaxation is caused by DD interactions mainly due to nearby ^{1}H nuclei. The extent of DD relaxation can be denoted using the relaxation rate, R_{1DD}. R_{1DD} was estimated with a method utilizing NOE. Measurement conditions: 9.4 T, 10 mM, 37 °C, D_2O. pD was adjusted to 7.4 ± 0.1 by DCl aq. or NaOD aq. See the detailed protocols described in the previous report.[19]

R_{1CSA} analysis

Chemical shift anisotropy (CSA) relaxation is caused by CSA of the nucleus and molecular tumbling. The extent of CSA relaxation can be denoted using the relaxation rate, R_{1CSA}. R_{1CSA} was estimated by measuring T_1 at various external magnetic field strength (9.4, 11.7, and 14.1 T) under thermal equilibrium state according to the previous reports.[20,21] R_{1CSA} contribution at 9.4 T was calculated using the following eqn (1).

$$R_{1CSA}(9.4\ T) = R_1(9.4\ T) - R_1(0\ T) \quad (1)$$

where R_1(0 T) is the *y*-axis intercept of R_1–$B_0{}^2$ plot in Fig. S1.†

Hyperpolarized experiments

General information on hyperpolarized studies. Hyperpolarization was achieved using a HyperSense DNP polarizer (Oxford Instruments, UK) with microwave irradiation at 93.938 GHz and 100 mW at 1.4 K. Subsequent ^{13}C NMR was acquired with a 1.4 T Spinsolve 60 Carbon High Performance benchtop NMR apparatus (Magritek, New Zealand).

Sample preparation for hyperpolarized experiments

To 82.5 mg of γ-Glu-[1-^{13}C]Gly was added 38 μL of 5 M NaOH aqueous solution, 60 μL of H_2O, and 15 μL of 10 M NaOH aqueous solution, successively. Similarly, to 81.6 mg of γ-Glu-[1-^{13}C]Gly-d_2 was added 38 μL of 5 M NaOH aqueous solution, 60 μL of H_2O, and 15 μL of 10 M NaOH aqueous solution, successively. After dissolving the probes, the final volumes became 180 μL for both γ-Glu-[1-^{13}C]Gly and γ-Glu-[1-^{13}C]Gly-d_2. Therefore, the final concentration of NaOH and the probes were 1.9 M and 2.2 M, respectively.

Hyperpolarized dynamic ^{13}C NMR

25 μL of 2.2 M γ-Glu-[1-^{13}C]Gly or γ-Glu-[1-^{13}C]Gly-d_2 in 1.9 M NaOH aqueous solution with 15 mM OX063 was hyperpolarized using the HyperSense DNP polarizer for 1 h. Hyperpolarized probe solution was acquired by the dissolution process with 3 mL of PBS containing 0.3 mM EDTA. 600 μL of hyperpolarized probe solution was used for acquiring dynamic ^{13}C NMR (flip

angle = 10°, repetition time = 4.5 s) with a 1.4 T Spinsolve 60 Carbon High Performance benchtop NMR apparatus.

Results and discussion

Validation of γ-Glu–Gly scaffold and ^{13}C-enrichment of C1 in Gly residue

Evaluation of GGT-mediated Glu production of peptide substrates. We initially evaluated Glu production by GGT from GSH, γ-Glu–Gly–Gly, and γ-Glu–Gly *in vitro*. We added beef kidney GGT to 5 mM GSH, γ-Glu–Gly–Gly, and γ-Glu–Gly in phosphate buffer (PB), which we assumed was close to the local probe concentration in DNP MRI. The samples were incubated at 37 °C for 30 or 60 min. We then determined the amounts of Glu generated as a hydrolytic product of GGT by mixing with 4-fluoro-7-nitrobenzofurazan and comparing the results of UHPLC with a calibration curve (Fig. 2). Each of GSH, γ-Glu–Gly–Gly, and γ-Glu–Gly produced Glu *via* hydrolysis catalyzed by GGT. We found that γ-Glu–Gly–Gly generated more Glu than GSH, a natural substrate of GGT and that γ-Glu–Gly–Gly and γ-Glu–Gly produced similar amounts of Glu. This implied that γ-Glu–Gly is a good dipeptide substrate that can achieve hydrolytic conversion comparable to that of tripeptides. The hyperpolarized state realized by d-DNP immediately decays back to thermal equilibrium after dissolution with T_1 as the time constant. Therefore, practical DNP molecular probes need to react fast enough with the target enzyme to produce a measurable amount of product within a few minutes. The finding that γ-Glu–Gly produced more Glu than the natural substrate GSH under our experimental conditions supports the notion that γ-Glu–Gly is a useful DNP probe from the viewpoint of enzymatic conversion.

Evaluation of magnetic properties of γ-[5-^{13}C]Glu–Gly, γ-Glu-[1-^{13}C]Gly, and their GGT-hydrolysis products. We investigated the appropriate ^{13}C-enrichment position for γ-Glu–Gly as a DNP probe. To realize hyperpolarized metabolic analysis *in vivo*, an isotope-enriched position needs to have a long T_1 and a large chemical shift change before and after the reaction. Many DNP probes utilize ^{13}C, which is a hetero nucleus with a small gyromagnetic ratio and thus a long T_1. Furthermore, since ^{1}H is not directly attached, quaternary carbons are useful for realizing long T_1 by avoiding relaxation due to DD interactions with nearby ^{1}H, which is generally the main relaxation source for ^{13}C.[22,23] γ-Glu–Gly has the three quaternary carbonyl carbons that would realize a long T_1. Among them, C5 of the Glu residue and C1 of the Gly residue are thought to induce a large chemical shift change upon GGT-mediated structural changes (Fig. 3A). Therefore, we focused on γ-[5-^{13}C]Glu–Gly, γ-Glu-[1-^{13}C]Gly (the conventional probe), and their GGT-hydrolysis products ([5-^{13}C]Glu and [1-^{13}C]Gly).

We prepared γ-[5-^{13}C]Glu–Gly according to Scheme S1.† The ^{13}C chemical shift of each probe/product in D_2O under neutral conditions was determined at 9.4 T using 1,4-dioxane (67.19 ppm) as an internal standard for ^{13}C NMR (Fig. 3B). The chemical shift differences between the probe and the product were 6.8 ppm for γ-[5-^{13}C]Glu–Gly/[5-^{13}C]Glu and 4.4 ppm for γ-Glu-[1-^{13}C]Gly/[1-^{13}C]Gly. The chemical shift change given by γ-Glu-[1-^{13}C]Gly/[1-^{13}C]Gly was distinguishable *in vivo*. The chemical shift change of 6.8 ppm by γ-[5-^{13}C]Glu–Gly/[5-^{13}C]Glu was even larger, suggesting that both pairs can clearly distinguish the hyperpolarized signals of the probe and the product.

We then evaluated the T_1 values of each probe and product at 9.4 T using inversion recovery (Fig. 3B). The T_1 of γ-[5-^{13}C]Glu–Gly was 13 ± 1 s (9.4 T, 10 mM, D_2O, 37 °C), and that of the corresponding product, [5-^{13}C]Glu, was 35 ± 1 s (9.4 T, 10 mM, D_2O, 37 °C). The T_1 value of the conventional probe, γ-Glu-[1-^{13}C]Gly, was 31 ± <1 s (9.4 T, 10 mM, D_2O, 37 °C), and that of the corresponding product, [1-^{13}C]Gly, was 56 ± 4 s (9.4 T, 10 mM, D_2O, 37 °C). The results of measuring the T_1 of γ-[5-^{13}C]Glu–Gly and γ-Glu-[1-^{13}C]Gly revealed that the T_1 of the carbonyl carbons in the same molecule can differ ~2-fold depending on the ^{13}C-labeling position (13 ± 1 *vs.* 31 ± <1 s). These results indicated that the chemical shift changes of both pairs of the probe and the product were sufficient (6.8 *vs.* 4.4 ppm), whereas the T_1 of γ-[5-^{13}C]Glu–Gly was much shorter than that of γ-Glu-[1-^{13}C]Gly (13 ± 1 *vs.* 31 ± <1 s). Therefore, γ-Glu-[1-^{13}C]Gly with the longer T_1, is the preferred DNP probe for detecting GGT because the probe must retain the hyperpolarized signal long enough to generate an obvious enzymatic reaction product.

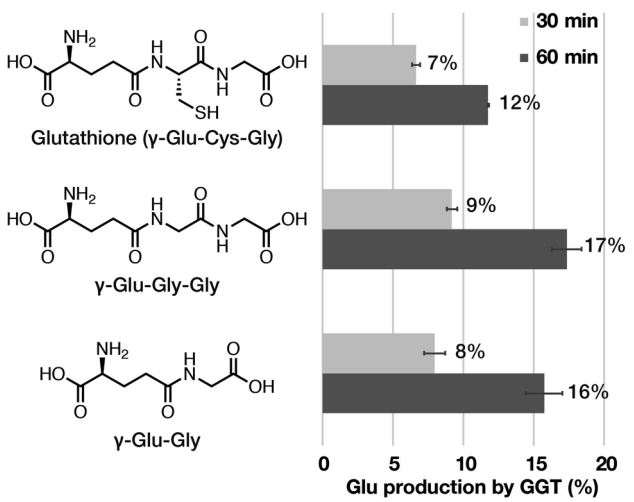

Fig. 2 Comparison of GGT-mediated enzymatic reaction among GSH (γ-Glu–Cys–Gly), γ-Glu–Gly–Gly, and γ-Glu–Gly. Glu production (%) was calculated as 100 × [Glu]/[initial substrate concentration, 5 mM] at the time point of 30 min and 60 min. Error bars represent standard deviation (n = 3).

Relaxation mechanism analysis of γ-Glu-[1-^{13}C]Gly and γ-Glu-[1-^{13}C]Gly-d_2

Synthesis of γ-Glu-[1-^{13}C]Gly-d_2. A detailed evaluation of the enzymatic reaction and the magnetic parameters of γ-Glu–Gly showed that γ-Glu-[1-^{13}C]Gly is a promising DNP probe for sensing GGT. In addition, in the previous report, we could detect the enzymatic conversion of a probe even *in vivo* using γ-Glu-[1-^{13}C]Gly. However, if the distance from the polarizer to the MRI or NMR apparatus is far, or if longer retention of the hyperpolarized signal is required for measurements, a deuterated γ-Glu-[1-^{13}C]Gly with an extended T_1 would be appropriate

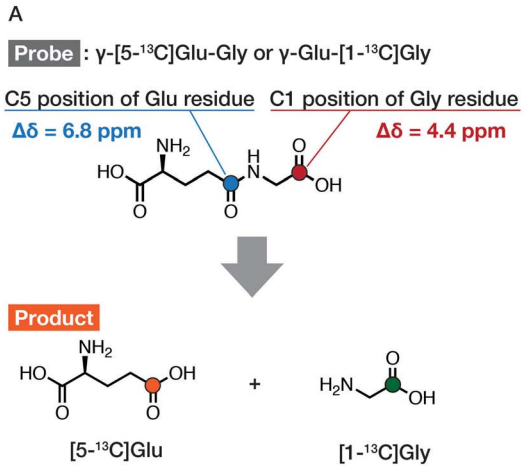

B

Compound	Chemical structure	T_1 (s)	Chemical shift (ppm)
γ-[5-^{13}C]Glu-Gly	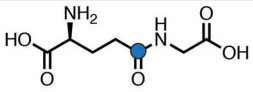	13 ± 1	175.1
[5-^{13}C]Glu	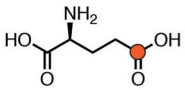	35 ± 1	181.9
γ-Glu-[1-^{13}C]Gly	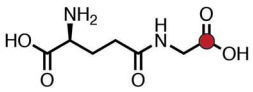	31 ± <1	177.3
[1-^{13}C]Gly	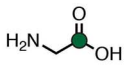	56 ± 4	172.9

Fig. 3 Potential ^{13}C-enriched positions of γ-Glu–Gly and its hydrolysis products, and the magnetic parameters of probes and products. (A) Potential ^{13}C-enriched positions of γ-Glu–Gly and its hydrolysis products, [5-^{13}C]Glu and [1-^{13}C]Gly. Colored atoms indicate isotope-enriched ^{13}C. Δδ is ^{13}C chemical shift difference between the probe and the product. (B) Chemical structures, T_1 values, and ^{13}C chemical shifts of probes and products. T_1 values were measured by inversion recovery (9.4 T, 10 mM, D_2O, 37 °C, pD = 7.4 ± 0.1). Error bars represent standard deviation (n = 3). ^{13}C Chemical shift was determined using 1,4-dioxane (67.19 ppm) as an internal standard (9.4 T, 5 mM, D_2O, 37 °C, pD = 7.4 ± 0.1).

to further extend the hyperpolarization lifetime of γ-Glu-[1-^{13}C]Gly.

We first investigated the T_1 relaxation effect of the α-^{1}H of the Gly residue of the probe (Fig. 4A). We synthesized γ-Glu-[1-^{13}C]Gly-d_2 as shown in Scheme 1. The quantitative *N*-hydroxyl succinimide (NHS) esterification proceeded using 1-ethyl-3-(3-dimethylaminopropyl)carbodiimide hydrochloride (EDCI·HCl) as a coupling agent. The NHS ester can be purified by extraction and recrystallization, and isolated in 99% yield. By coupling of the NHS ester with [1-^{13}C]Gly-d_2,[24] *N*-Cbz-γ-Glu(OBn)-[1-^{13}C]Gly-d_2 was synthesized. γ-Glu-[1-^{13}C]Gly-d_2 was then obtained *via* hydrogenation to deprotect Cbz and Bn groups. Details of the synthetic procedure are described in the Experimental section. This scheme can provide sufficient amounts (gram scale) of γ-Glu-[1-^{13}C]Gly and γ-Glu-[1-^{13}C]Gly-d_2.

T_1 measurements of γ-Glu-[1-^{13}C]Gly and γ-Glu-[1-^{13}C]Gly-d_2 under various solvent conditions

The T_1 of γ-Glu-[1-^{13}C]Gly and γ-Glu-[1-^{13}C]Gly-d_2 was evaluated at 9.4 T under various solvent conditions. In the previous report, only the T_1 at 25 °C in H_2O has been reported. However, T_1

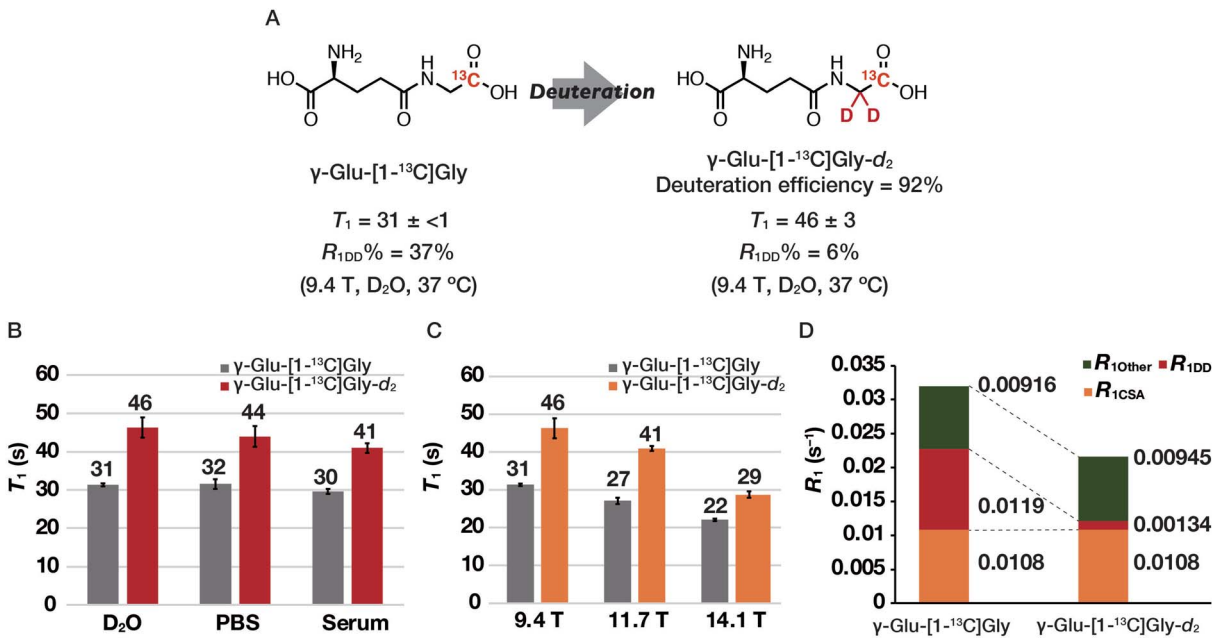

Fig. 4 Chemical structures, T_1 values, and T_1 relaxation analysis of γ-Glu-[1-^{13}C]Gly and γ-Glu-[1-^{13}C]Gly-d_2. (A) Chemical structures of γ-Glu-[1-^{13}C]Gly and γ-Glu-[1-^{13}C]Gly-d_2. (B) T_1 measurements of γ-Glu-[1-^{13}C]Gly and γ-Glu-[1-^{13}C]Gly-d_2 in D_2O, PBS, and serum containing 10% D_2O (9.4 T, 10 mM, 37 °C). (C) T_1 measurements of γ-Glu-[1-^{13}C]Gly and γ-Glu-[1-^{13}C]Gly-d_2 in D_2O at 9.4, 11.7, and 14.1 T. Error bars represent standard deviation (n = 3). (D) T_1 relaxation analysis of γ-Glu-[1-^{13}C]Gly and γ-Glu-[1-^{13}C]Gly-d_2 in D_2O at 9.4 T.

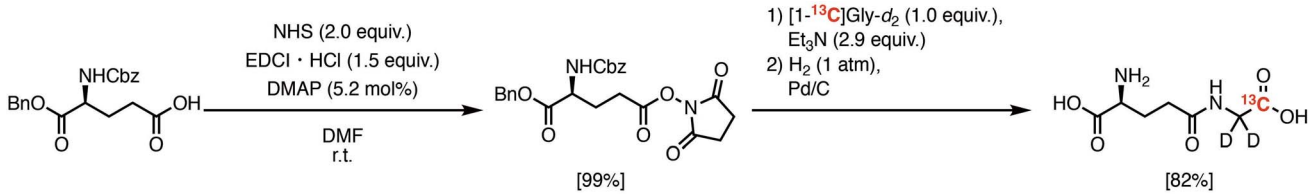

Scheme 1 Synthetic scheme of γ-Glu-[1-^{13}C]Gly-d_2.

values in PBS and serum are also important for DNP NMR/MRI experiments because hyperpolarized probes are often dissolved in aqueous buffers and circulate in biological media to reach a target site after administration *in vivo*. Thus, we measured the T_1 of γ-Glu-[1-^{13}C]Gly and γ-Glu-[1-^{13}C]Gly-d_2 at 9.4 T in D_2O, PBS, and serum (Fig. 4B). The results showed that even in mouse serum, the T_1 was 30 ± 1 s for γ-Glu-[1-^{13}C]Gly and 41 ± 1 s for γ-Glu-[1-^{13}C]Gly-d_2 (9.4 T, 10 mM, mouse serum with 10% D_2O, 37 °C), which was comparable to that in D_2O. These results suggested that the hyperpolarization lifetime of these probes should be sufficient, even in a biological environment.

T_1 and R_{1DD} analysis of γ-Glu-[1-^{13}C]Gly and γ-Glu-[1-^{13}C]Gly-d_2

We measured the T_1 of γ-Glu-[1-^{13}C]Gly-d_2 to determine the DD relaxation effect of the α-^{1}H of the Gly residue (Fig. 4A). The deuteration efficiency of γ-Glu-[1-^{13}C]Gly-d_2 was 92% and the T_1 was 46 ± 3 s (9.4 T, 10 mM, D_2O, 37 °C). Deuteration of the α-^{1}H of the Gly residue in γ-Glu-[1-^{13}C]Gly resulted in a 1.5-fold longer T_1 (46 ± 3 *vs.* 31 ± <1 s).

We investigated how α-deuteration of the Gly residue reduced the contribution of DD relaxation of the probe to overall T_1 relaxation (Fig. 4A). The relaxation rate of the nucleus, R_1 (=1/T_1), is described as the sum of the contributions from independent relaxation factors as denoted in eqn (2).[25,26]

$$\frac{1}{T_1} = R_1 = R_{1DD} + R_{1CSA} + R_{1Other} \quad (2)$$

where R_{1DD} is a relaxation due to DD interaction mainly caused by nearby ^{1}H, R_{1CSA} is a relaxation due to CSA, and R_{1Other} is a component from all other relaxations including scalar coupling, spin rotation, and relaxation by paramagnetic agents. R_{1DD} and R_{1CSA} typically account for most of the R_1 of ^{13}C nuclei at high magnetic fields. We then estimated the ^{1}H–^{13}C R_{1DD} contributions of γ-Glu-[1-^{13}C]Gly and γ-Glu-[1-^{13}C]Gly-d_2 using the nuclear Overhauser effect.[19,26–30] We found that 37% of the total R_1 of γ-Glu-[1-^{13}C]Gly was responsible for DD relaxation at 9.4 T, whereas only 6% of that of γ-Glu-[1-^{13}C]Gly-d_2 was responsible for DD. Because the R_{1DD} of γ-Glu-[1-^{13}C]Gly-d_2, in which only the α-^{1}Hs of the Gly residue were deuterated, decreased to 6%, most of the DD relaxation of γ-Glu-[1-^{13}C]Gly was caused by the α-^{1}H of the Gly residue. The findings that the α-^{1}H near the ^{13}C nucleus of γ-Glu-[1-^{13}C]Gly accounted for most of the DD relaxation is consistent with the theoretical explanation that the R_{1DD} is inversely proportional to the sixth power of the distance between the ^{1}H and ^{13}C nuclei.[25,26] These findings showed that γ-Glu-[1-^{13}C]Gly-d_2 suppressed most of the DD relaxation and resulted in a 1.5-fold longer T_1 than the conventional probe at 9.4 T.

Analysis of R_{1CSA} and T_1 measurements of γ-Glu-[1-^{13}C]Gly and γ-Glu-[1-^{13}C]Gly-d_2 at various magnetic field strengths

We measured the T_1 of γ-Glu-[1-^{13}C]Gly and γ-Glu-[1-^{13}C]Gly-d_2 at 9.4, 11.7, and 14.1 T to determine the contribution of the magnetic field-dependent relaxation pathway. The CSA relaxation mechanism increases in proportion to the square of the external magnetic field strength (B_0).[20,21] Assuming that magnetic field-dependent relaxation mechanisms other than CSA are negligible, R_{1CSA} can be estimated by examining the magnetic field dependence of T_1. The results of the T_1 measurements of γ-Glu-[1-^{13}C]Gly and γ-Glu-[1-^{13}C]Gly-d_2 in D_2O at 9.4, 11.7, and 14.1 T showed that T_1 tends to become shorter with increasing magnetic field strengths of 9.4, 11.7, and 14.1 T (γ-Glu-[1-^{13}C]Gly: 31 ± <1, 27 ± 1, and 22 ± <1 s respectively; γ-Glu-[1-^{13}C]Gly-d_2: 46 ± 3, 41 ± 1, and 29 ± 1 s, respectively; Fig. 4C). This is because relaxation due to CSA increases at higher magnetic field strength, and results in a shorter T_1. The contribution of R_{1CSA} to total R_1 calculated from the R_1–B_0^2 plot in D_2O was 34% for γ-Glu-[1-^{13}C]Gly at 9.4 T (Fig. 4D and S1†). This result is consistent with the fact that carbonyl ^{13}C generally exhibits a large relaxation due to the CSA mechanism.[22] Together with the results of the R_{1DD} analysis, 71% of the relaxation pathway of γ-Glu-[1-^{13}C]Gly at 9.4 T was accounted for by the DD and CSA relaxation mechanisms (Fig. 4D).

Relaxation due to the DD and CSA mechanisms must be reduced to further extend the hyperpolarization signal lifetime of γ-Glu-[1-^{13}C]Gly. The DD relaxation can be reduced to 6% by deuterating the α-^{1}H of the Gly residue of γ-Glu-[1-^{13}C]Gly. In addition, the contribution of R_{1CSA} can be reduced by a lower magnetic field strength, meaning that the hyperpolarization signal lifetime of both γ-Glu-[1-^{13}C]Gly and γ-Glu-[1-^{13}C]Gly-d_2 should be extended in a lower magnetic field along with the longer T_1. Especially, γ-Glu-[1-^{13}C]Gly-d_2 should realize the longer T_1 and thus the longer retention of the hyperpolarized signal at lower magnetic field by reducing both R_{1DD} and R_{1CSA}.

Dynamic ^{13}C NMR spectra of hyperpolarized γ-Glu-[1-^{13}C]Gly and γ-Glu-[1-^{13}C]Gly-d_2 at 1.4 T

We acquired dynamic ^{13}C NMR spectra of hyperpolarized γ-Glu-[1-^{13}C]Gly and γ-Glu-[1-^{13}C]Gly-d_2 at 1.4 T to demonstrate the utility of the deuterated probe for further T_1 elongation by reducing both R_{1DD} and R_{1CSA}. We hyperpolarized γ-Glu-[1-^{13}C]Gly under the condition without glassing reagents (2.2 M γ-Glu-

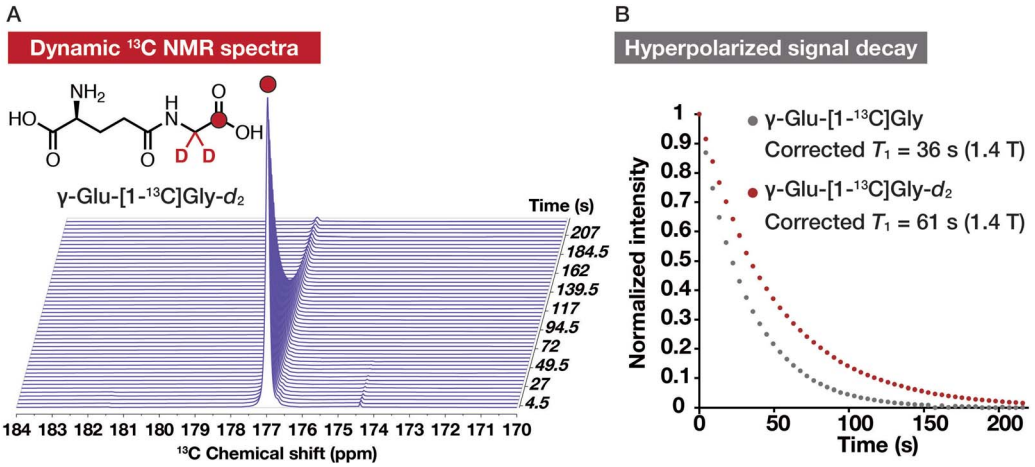

Fig. 5 Monitoring of the hyperpolarized ^{13}C NMR signal decay of γ-Glu-[1-^{13}C]Gly-d_2 and γ-Glu-[1-^{13}C]Gly at 1.4 T. (A) Dynamic ^{13}C NMR spectra of hyperpolarized γ-Glu-[1-^{13}C]Gly-d_2 at 1.4 T. Colored atoms indicate isotope-enriched ^{13}C. (B) Hyperpolarized signal decays of γ-Glu-[1-^{13}C]Gly-d_2 and γ-Glu-[1-^{13}C]Gly and their corrected T_1 at 1.4 T.

[1-^{13}C]Gly in 1.9 M NaOH with 15 mM OX063) using the HyperSense DNP polarizer. After dissolving the cryogenic sample by 3 mL of PBS containing 0.3 mM EDTA, hyperpolarized γ-Glu-[1-^{13}C]Gly solution (600 μL) was used to acquire dynamic ^{13}C NMR spectra with a 1.4 T benchtop NMR apparatus. γ-Glu-[1-^{13}C]Gly-d_2 was also hyperpolarized with the same procedure. Both of the probes gave the enhanced ^{13}C NMR signals (Fig. 5A and S2†). T_1 of γ-Glu-[1-^{13}C]Gly-d_2 calculated from the hyperpolarized signal decay was 61 s at 1.4 T (corrected T_1 considering magnetic loss during successive acquisition pulses), which was longer than that of γ-Glu-[1-^{13}C]Gly (36 s, Fig. 5B). As we expected, γ-Glu-[1-^{13}C]Gly-d_2 showed the longer T_1 at 1.4 T than 9.4 T (44 ± 3 s at 9.4 T *vs.* 61 s at 1.4 T). The experimentally obtained T_1 value of γ-Glu-[1-^{13}C]Gly-d_2 (61 s at 1.4 T) was shorter than the extrapolated value from the R_1–B_0^2 plot in D_2O (101 s at 1.4 T, Fig. S1†). The reason the experimentally determined T_1 (61 s at 1.4 T, corrected) calculated from the signal decay curve is shorter than the extrapolated T_1 (101 s at 1.4 T) might be explained by coexisting radicals, which are included during the hyperpolarization process. These results, however, indicated that γ-Glu-[1-^{13}C]Gly-d_2 is a DNP probe that has a longer T_1 than γ-Glu-[1-^{13}C]Gly and thus achieves a longer hyperpolarization signal lifetime at 1.4 T.

Conclusions

In this study, we evaluated the enzymatic and magnetic properties of γ-Glu-[1-^{13}C]Gly and developed the deuterated probe, γ-Glu-[1-^{13}C]Gly-d_2 that can show the longer T_1 and thus the longer lifetime of the hyperpolarized signal. We found that (1) γ-Glu–Gly showed a rapid enzymatic reaction rate with GGT, (2) γ-Glu-[1-^{13}C]Gly showed a longer T_1 than γ-[5-^{13}C]Glu–Gly, another potential ^{13}C-enriched γ-Glu–Gly, (3) 71% of the T_1 relaxation of γ-Glu-[1-^{13}C]Gly can be accounted for by the DD and CSA relaxation pathway at 9.4 T, thus allowing T_1 elongation by deuteration and lower magnetic field strength, and that (4) γ-Glu-[1-^{13}C]Gly-d_2 indeed showed longer retention of the hyperpolarized signal at 1.4 T. These results confirmed the value of γ-Glu-[1-^{13}C]Gly-d_2 as a new DNP probe for detecting GGT with a longer lifetime of the hyperpolarized signal. Furthermore, the molecular properties of γ-Glu-[1-^{13}C]Gly-d_2 determined herein suggested that γ-Glu-[1-^{13}C]Gly-d_2 could be useful for biological studies of GGT.

Although the extended hyperpolarization lifetime was demonstrated *in vitro*, *in vivo* verification experiments were not tried in this study. The feasibility of the elongated hyperpolarized signal of the deuterated probe *in vivo* should be investigated in future studies. In addition, there may still be room for further improvement in the molecular design of γ-Glu-[1-^{13}C]Gly before the applications of γ-Glu-[1-^{13}C]Gly could be more widened and significantly contribute to hyperpolarized MR studies. For example, the GGT enzymatic reaction rate of γ-Glu-[1-^{13}C]Gly might still be able to be improved, because γ-Glu-[1-^{13}C]Gly provided only a few percent of the product/probe ratio in the previous *in vivo* experiments using tumor-bearing xenografts.[15,17] DNP probes that can detect GGT with better conversion could be developed by understanding the enzymatic reaction mechanism of GGT.

We believe that the enzymatic properties and various magnetic parameters of γ-Glu-[1-^{13}C]Gly and γ-Glu-[1-^{13}C]Gly-d_2 determined herein will provide useful information for widespread use as a DNP probe for GGT detection in biological studies, and insights for the development of DNP probes designed *de novo* in the future.

Author contributions

S. S. conceived and designed the project; Y. K., T. N., and M. I. synthesized compounds with the help of Y. S. and H. N.; Y. K. conducted *in vitro* enzymatic reaction assay and NMR measurements for T_1, chemical shift, and relaxation analysis with the help of Y. S.; A. E. E., F. H., and M. M. organized and/or performed the hyperpolarized experiments; Y. K., Y. S., and S. S. wrote the manuscript, which was edited by all co-authors.

Conflicts of interest

There are no conflicts of interest to declare.

Acknowledgements

This research was supported by MEXT Q-LEAP [grant number JPMXS0120330644 (to S. S.)]; JSPS KAKENHI [grant numbers JP19H00919 (to S. S.); JP20K15396 (to Y. S.); JP19J22848 (to Y. K.)]; and JSPS Fostering Joint International Research (B) [grant number JP20KK0253 (to F. H. and M. M.)]. We thank Ms Keiko Ideta (Evaluation Center of Materials Properties and Function, Institute for Materials Chemistry and Engineering, Kyushu University) for support with the NMR measurements.

References

1 J. W. Keillor, R. Castonguay and C. Lherbet, *Methods Enzymol.*, 2005, **401**, 449–467.
2 V. I. Lushchak, *J. Amino Acids*, 2012, **2012**, 1–26.
3 M. H. Hanigan, *Adv. Cancer Res.*, 2014, **122**, 103–141.
4 H. Khurana, V. K. Meena, S. Prakash, K. Chuttani, N. Chadha, A. Jaswal, D. K. Dhawan, A. K. Mishra and P. P. Hazari, *PLoS One*, 2015, **10**, 1–20.
5 D. Gao, Y. Miao, S. Ye, C. Lu, G. Lv, K. Li, C. Yu, J. Lin and L. Qiu, *RSC Adv.*, 2021, **11**, 18738–18747.
6 Z. Luo, R. An and D. Ye, *ChemBioChem*, 2019, **20**, 474–487.
7 Y. Urano, M. Sakabe, N. Kosaka, M. Ogawa, M. Mitsunaga, D. Asanuma, M. Kamiya, M. R. Young, T. Nagano, P. L. Choyke and H. Kobayashi, *Sci. Transl. Med.*, 2011, **3**, 1–11.
8 J. H. Ardenkjær-Larsen, B. Fridlund, A. Gram, G. Hansson, L. Hansson, M. H. Lerche, R. Servin, M. Thaning and K. Golman, *Proc. Natl. Acad. Sci. U. S. A.*, 2003, **100**, 10158–10163.
9 A. Comment, *J. Magn. Reson.*, 2016, **264**, 39–48.
10 Z. J. Wang, M. A. Ohliger, P. E. Z. Larson, J. W. Gordon, R. A. Bok, J. Slater, J. E. Villanueva-Meyer, C. P. Hess, J. Kurhanewicz and D. B. Vigneron, *Radiology*, 2019, **291**, 273–284.
11 J. Kurhanewicz, D. B. Vigneron, J. H. Ardenkjaer-Larsen, J. A. Bankson, K. Brindle, C. H. Cunningham, F. A. Gallagher, K. R. Keshari, A. Kjaer, C. Laustsen, D. A. Mankoff, M. E. Merritt, S. J. Nelson, J. M. Pauly, P. Lee, S. Ronen, D. J. Tyler, S. S. Rajan, D. M. Spielman, L. Wald, X. Zhang, C. R. Malloy and R. Rizi, *Neoplasia*, 2019, **21**, 1–16.
12 M. Fiedorowicz, M. Wieteska, K. Rylewicz, B. Kossowski, E. Piatkowska-Janko, A. M. Czarnecka, B. Toczylowska and P. Bogorodzki, *Biocybern. Biomed. Eng.*, 2021, **41**, 1466–1485.
13 T. Nishihara, H. A. I. Yoshihara, H. Nonaka, Y. Takakusagi, F. Hyodo, K. Ichikawa, E. Can, J. A. M. Bastiaansen, Y. Takado, A. Comment and S. Sando, *Angew. Chem., Int. Ed.*, 2016, **55**, 10626–10629.
14 S. F. Frank, H. A. Yoshihara, M. Itoda, S. Sando and R. Gruetter, *Proc. Intl. Mag. Reson. Med.*, 2018, **26**, 3066.
15 T. Seki, M. Itoda, S. Kishimoto, K. Yamamoto, Y. Takakusagi, J. Brender, R. M. Malinowski, T. Nishihara, H. A. I. Yoshihara, H. Nonaka, K. Saito, N. Oshima, J. H. Ardenkjaer-Larsen, J. B. Mitchell, M. C. Krishna and S. Sando, *Proc. Intl. Mag. Reson. Med.*, 2018, **26**, 3052.
16 G. Batsios, C. Najac, P. Cao, P. Viswanath, E. Subramani, Y. Saito, A. M. Gillespie, H. A. I. Yoshihara, P. Larson, S. Sando and S. M. Ronen, *Sci. Rep.*, 2020, **10**, 6244.
17 T. Seki, K. Yamamoto, N. Oshima, M. Itoda, Y. Kondo, Y. Saito, Y. Takakusagi, S. Kishimoto, J. Brender, R. M. Malinowski, J. H. Ardenkjær-Larsen, H. Nonaka, M. C. Krishna and S. Sando, *Proc. Intl. Mag. Reson. Med.*, 2020, **28**, 3032.
18 M. R. Molla, P. Prasad and S. Thayumanavan, *J. Am. Chem. Soc.*, 2015, **137**, 7286–7289.
19 Y. Imakura, H. Nonaka, Y. Takakusagi, K. Ichikawa, N. R. Maptue, A. M. Funk, C. Khemtong and S. Sando, *Chem.–Asian J.*, 2018, **13**, 280–283.
20 T. D. Alger, W. D. Hamill, R. J. Pugmire, D. M. Grant, G. D. Siltcox and M. Solum, *J. Phys. Chem.*, 1980, **84**, 632–636.
21 T. C. Wong, T. T. Ang, F. S. Guziec and C. A. Moustakis, *J. Magn. Reson.*, 1984, **57**, 463–470.
22 K. R. Keshari and D. M. Wilson, *Chem. Soc. Rev.*, 2014, **43**, 1627–1659.
23 Y. Kondo, H. Nonaka, Y. Takakusagi and S. Sando, *Angew. Chem., Int. Ed.*, 2021, **60**, 14779–14799.
24 C. Taglang, D. E. Korenchan, C. von Morze, J. Yu, C. Najac, S. Wang, J. E. Blecha, S. Subramaniam, R. Bok, H. F. VanBrocklin, D. B. Vigneron, S. M. Ronen, R. Sriram, J. Kurhanewicz, D. M. Wilson and R. R. Flavell, *Chem. Commun.*, 2018, **54**, 5233–5236.
25 E. D. Becker, R. R. Shoup and T. C. Farrar, *Pure Appl. Chem.*, 1972, **32**, 51–66.
26 G. C. Levy, *Acc. Chem. Res.*, 1973, **6**, 161–169.
27 E. Breitmaier, K. H. Spohn and S. Berger, *Angew. Chem., Int. Ed.*, 1975, **14**, 144–159.
28 K. F. Kuhlmann and D. M. Grant, *J. Am. Chem. Soc.*, 1968, **90**, 7355–7357.
29 G. C. Levy, J. D. Cargioli and F. A. L. Anet, *J. Am. Chem. Soc.*, 1973, **95**, 1527–1535.
30 D. Gust, H. Pearson, I. M. Armitage and J. D. Roberts, *J. Am. Chem. Soc.*, 1976, **98**, 2723–2726.